Flexible Photonic Cellulose Nanocrystal Films

Giulia Guidetti, Siham Atifi, Silvia Vignolini, and Wadood Y. Hamad**

Cellulose is an abundant and sustainable biopolymer that has gained renewed interest in materials science.[1] It is produced in the cell wall of many plants via condensation polymerization of glucose and provides structural integrity and protection.[2] Functional materials synthesized from nanocellulose (nanofibers and nanocrystals) show promise in many potential applications such as sensing,[3] catalyst supports,[4] nanofiltration,[5] tissue engineering,[6] electronics,[7] and solar energy harvesting.[8]

The supramolecular structure of cellulose includes crystalline and amorphous domains.[10a] Among the various forms of cellulosic building blocks, cellulose nanocrystals (CNCs) are of particular interest for materials development.[9] CNCs can be obtained by controlled acid hydrolysis of cellulosic biomass, yielding spindle-shaped nanocrystals on the order of 5–20 nm in diameter and a few hundred nanometers in length.[11,12] The Young's modulus of a single crystal has been experimentally determined, using Raman microscopy, to be over 140 GPa.[13] Hydrolysis using sulfuric (or phosphoric) acid generates sulfate (or phosphate) ester groups on the CNC surface that are crucial for the stabilization of aqueous colloidal suspensions of CNCs.[10b,11,12] Significantly, sulfate-functionalized CNCs organize into a chiral nematic lyotropic liquid crystalline (LLC) phase,[11] and upon slow evaporation of water, the organization of CNCs present in the LLC phase can be retained in solid films endowing the resulting materials with a helicoidal structure and brilliant iridescent (structural) colors.[14] This property has been utilized to embed chiral nematic structures into silica,[15] organosilica,[16] hydrogels,[17] thermoset phenol-formaldehyde (PF)[18a] and amino-formaldehyde resins.[18b] In some cases, the selective removal of CNCs as sacrificial templates resulted in mesoporous silica,[15] organosilica,[16] and PF resins[18]—materials with high surface areas and well-ordered helicoidal pores. Moreover, it has recently been demonstrated that a co-templating approach can be used to construct porous cellulosic materials with photonic properties in a multi-step synthesis procedure. Selective removal of the space-filling resin from a urea-formaldehyde/CNC composite resulted in porous photonic membranes comprised entirely of CNCs.[19]

The optical response of structures comprising a nanoscale internal arrangement depends on the properties of the nanoscale building blocks and on the parameters that determine their assembly into a macroscopic structure,[20–22] including temperature,[23] the substrate material,[24] and the surface chemistry of the nanocrystals.[25,26] While the colloidal assembly of cellulose is robust and can be coupled with a range of chemical processes to form, for instance, composite materials with interesting optical properties,[15–19] the high mechanical performance of CNCs can be a drawback in some applications. Specifically, structurally colored films obtained via evaporation-induced self-assembly (EISA) are brittle, and thus unsuitable for applications requiring structural integrity and coherence in films or coatings. Attempts have been made to mix CNCs with water-soluble polymers to produce flexible and birefringent composites, for instance, sodium polyacrylate and poly(ethylene glycol),[27] poly(vinyl alcohol) and styrene-butadeine[28] or cellulose nanofibrils.[29] However, the incorporation of hydrophilic polymers, and cellulose nanocrystals, can limit the range and scope of iridescence, and can restrict their chiral nematic organization within the hydrophilic polymer matrix, or fibrous network.

Here we propose a novel, facile and scalable approach based on the co-assembly of zwitterionic (Zw) surfactants with CNCs resulting, upon evaporation, in flexible, iridescent films with tunable and controllable chiral nematic order. The zwitterionic surfactants electrostatically interact with the CNCs surface charge and act as springs connecting neighboring CNCs, thus creating a flexible net over which the CNCs can self-assemble and exhibit (unhindered) structural color. The photonic properties of the films have been carefully and extensively analyzed, and details of the results will be presented in this paper.

Samples with various mass ratio of CNC:dimethylmyristylammonio)propanesulfonate (DMAPS) and counterion were prepared: three samples with Na^+ as counter ions (NaCNC01, NaCNC041, and NaCNC1) and increasing surfactant content, as well as one with H^+ (HCNC041) as the counter ion, with a similar CNC:DMAPS mass ratio. The amount of Zw surfactant (DMAPS) was determined by gravimetry on the final dry films and confirmed by elemental analysis of the nitrogen and sulfur contents, **Table 1**. For samples NaCNC041 and HCNC041, both of same CNC:DMAPS mass ratio of 1:0.41, the nitrogen content was measured as 0.58% and 0.61%, respectively, which is identical within the margin of error associated with elemental measurements. When the CNC:DMAPS ratio was increased to 1:1, (sample NaCNC1) the nitrogen content was found to be 1.51%. The typical CNC nitrogen content in the control sample, NaCNC0, is less than 0.3% and undetectable via elemental analysis. The sulfur

G. Guidetti, Dr. S. Vignolini
Department of Chemistry
Cambridge University
Lensfield Road, Cambridge CB2 1EW, UK
E-mail: sv319@cam.ac.uk
Dr. S. Atifi, Dr. W. Y. Hamad
FPInnovations
2665 East Mall, Vancouver BC V6T 1Z4, Canada
E-mail: wadood.hamad@fpinnovations.ca

DOI: 10.1002/adma.201603386

ADVANCED MATERIALS
www.advmat.de

www.MaterialsViews.com

Table 1. Elemental analysis and conductivity data for CNC films prepared at different zwitterionic surfactant ratios.

Sample	CNC:DMAPS mass ratio	pH	Conductivity [μS cm^{-1}]	DMAPS [wt%]	C [%]	H [%]	N [%]	S [%]
NaCNC01	1:0.1	4.03	103	≤5	37.9	5.65	<0.3	0.64
NaCNC041	1:0.41	4.17	79	22	43.5	6.70	0.58	1.69
NaCNC1	1:1	4.23	75	53	46.7	7.74	1.51	3.63
HCNC041	1:0.41	3.04	319	19	43.1	6.66	0.61	1.44
NaCNC0	1:0	6.9	377	0	40.2	5.99	<0.3	0.68

content measurement in Table 1 further supports the successful ionic adsorption of DMAPS onto the CNC surface. For samples NaCNC041, NaCNC1, and HCNC041, the sulfur content was 1.69%, 3.63%, and 1.44%, respectively. A sulfur content[10b,12] of 0.68% for the control sample (NaCNC0) is typical for CNC extracted using sulfuric acid hydrolysis. The results suggest that any anionic form of sulfated CNCs can be reacted with the Zw surfactant to generate flexible, iridescent CNC films.

Figure 1a illustrates the mechanism of interaction between CNC suspensions with a zwitterionic surfactant, DMAPS. After the acid hydrolysis treatment with H_2SO_4, used to isolate the crystalline parts, some of the primary OH groups of the native cellulose are substituted with (negative) sulfate groups on the surface (−S−O_3^-), allowing the CNC to be well suspended in water. As DMAPS contains both negative (SO_3^-) and positive (N^+) centers, we expect that the N^+ from DMAPS is ionically adsorbed to the SO_3^- on the CNC surface, resulting in a net negative charge onto the CNC-DMAPS complex. Fourier transform infrared (FT-IR) spectra (Figure 1b,c) and ^{1}H NMR (Figure S1, Supporting Information, ESI) confirm the presence of DMAPS within the CNC-DMAPS complexes. As expected, the addition of DMAPS does not change the CNC structure,

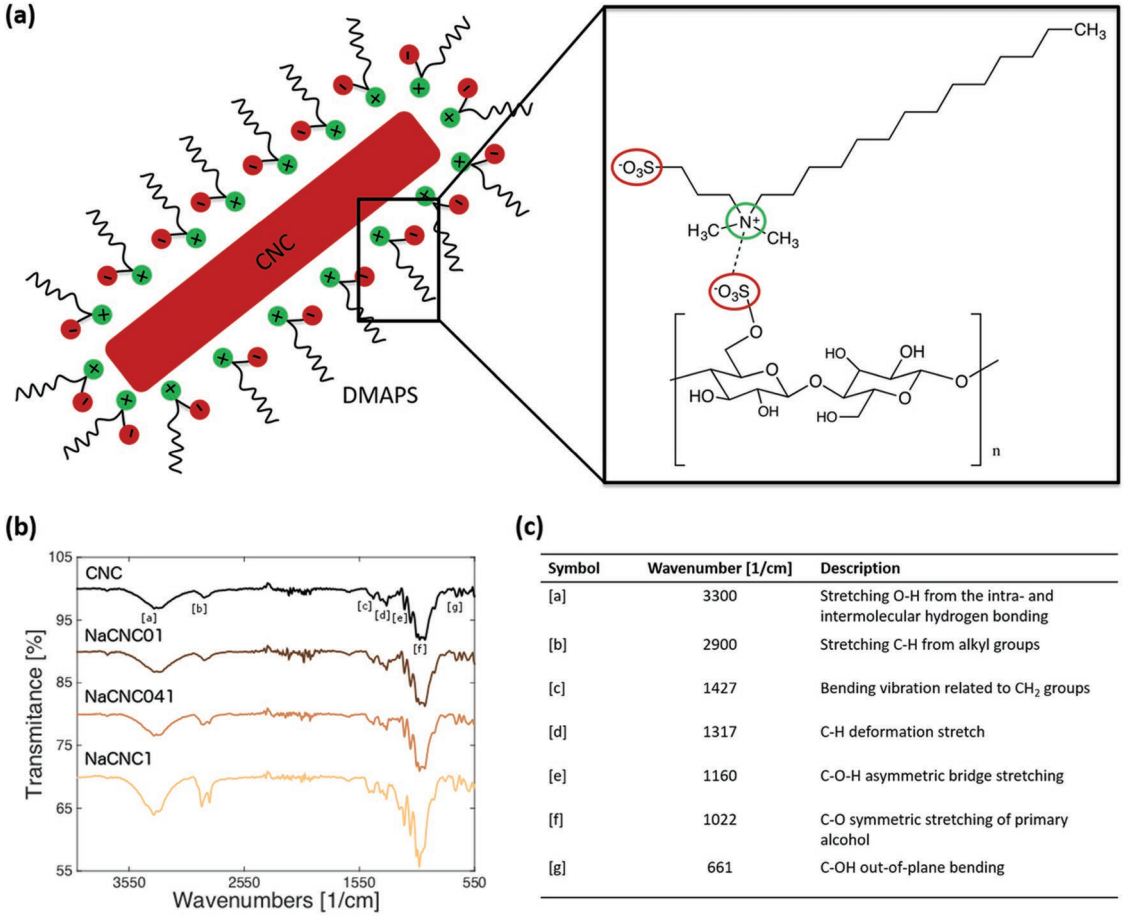

Symbol	Wavenumber [1/cm]	Description
[a]	3300	Stretching O-H from the intra- and intermolecular hydrogen bonding
[b]	2900	Stretching C-H from alkyl groups
[c]	1427	Bending vibration related to CH_2 groups
[d]	1317	C-H deformation stretch
[e]	1160	C-O-H asymmetric bridge stretching
[f]	1022	C-O symmetric stretching of primary alcohol
[g]	661	C-OH out-of-plane bending

Figure 1. a) Binding mechanism of the DMAPS surfactant onto the CNC surface, not drawn to scale, (left) with corresponding chemical structure (right). b) FTIR spectra of pure CNC and zwitterionic surfactant-CNC films prepared at 1:0.1, 1:0.41, and 1:1 CNC:DMAPS mass ratios. Increasing DMAPS dosage is qualitatively reflected with increasing intensity at ≈2900 cm^{-1}, which is responsible for C−H stretching from alkyl groups. This, along with the NMR results presented in Figure S1 in the Supporting Information, give reasonable and systematic confirmation of DMAPS adsorption to the CNC surfaces at evaluated mass ratios. Assignments of relevant bands [a]–[g] are shown in accompanying Table (c).

Adv. Mater. **2016**,
DOI: 10.1002/adma.201603386

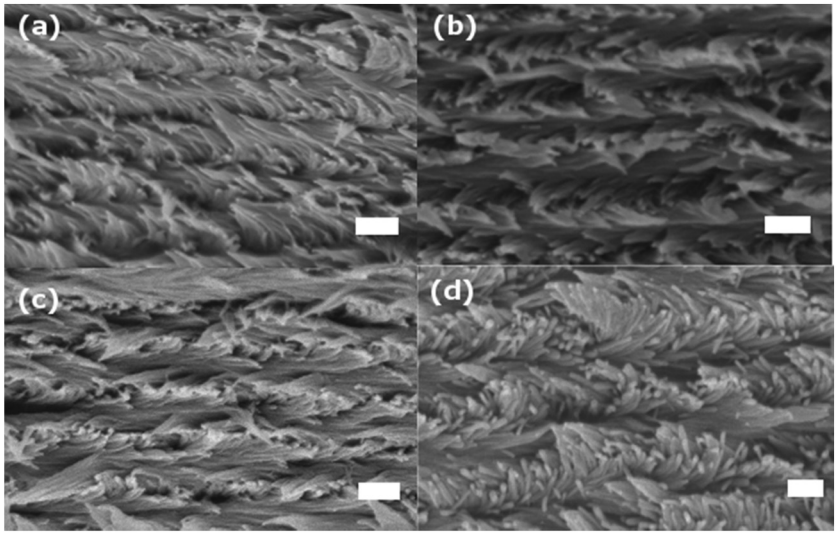

Figure 2. SEM images depicting chiral nematic organization of a) pure CNC and DMAPS:CNC films prepared at b) 1:0.1, c) 1:0.41, and d) 1:1 CNC:DMAPS mass ratios. Scale bars are 200 nm.

as evidenced by powder X-ray diffractometry (Figure S2, Supporting Information, ESI).

CNCs suspensions treated with Zw surfactants remains essentially hydrophilic. They are therefore dispersible in polar protic solvents, like water, and some polar aprotic solvents, like *N*,*N*-dimethylformamide, but not in non-polar solvents, like toluene or chloroform (Figure S3, Supporting Information, ESI). The physical sizes of the CNC nanoparticles used in this work were measured using atomic force microscopy (AFM), and are about 100 nm in length and 3.8 nm in height, standard deviation 70 and 2 nm (Figure S4, Supporting Information, ESI). However, the apparent nanoparticle diameter, as measured using dynamic light scattering,[30] is 50.5 ± 0.4 nm for pure CNC relative to the CNC-DMAPS complexes which measured 51.8 ± 1.3 nm for the 1:0.41 ratio (NaCNC041) and 53.2 ± 1.7 nm for the 1:1 ratio (NaCNC1). This indicates there is no significant change in particle size upon reacting with the Zw surfactant. Moreover, the presence of the surfactant does not prevent the assembly of the CNCs into a chiral nematic structure, as presented in the SEM images of **Figure 2** that clearly illustrate the Bouligand pattern typical of the helicoidal arrangement of CNCs.

The chiral nematic architecture of the film is also confirmed by polarized optical microscopy (**Figure 3**). For all the investigated samples we observe reflection of only left-circularly polarized light. The optical micrographs and the spectra presented in Figure 3 further confirm the shift towards higher wavelengths as the Zw surfactant ratios were increased relative to pure CNC.

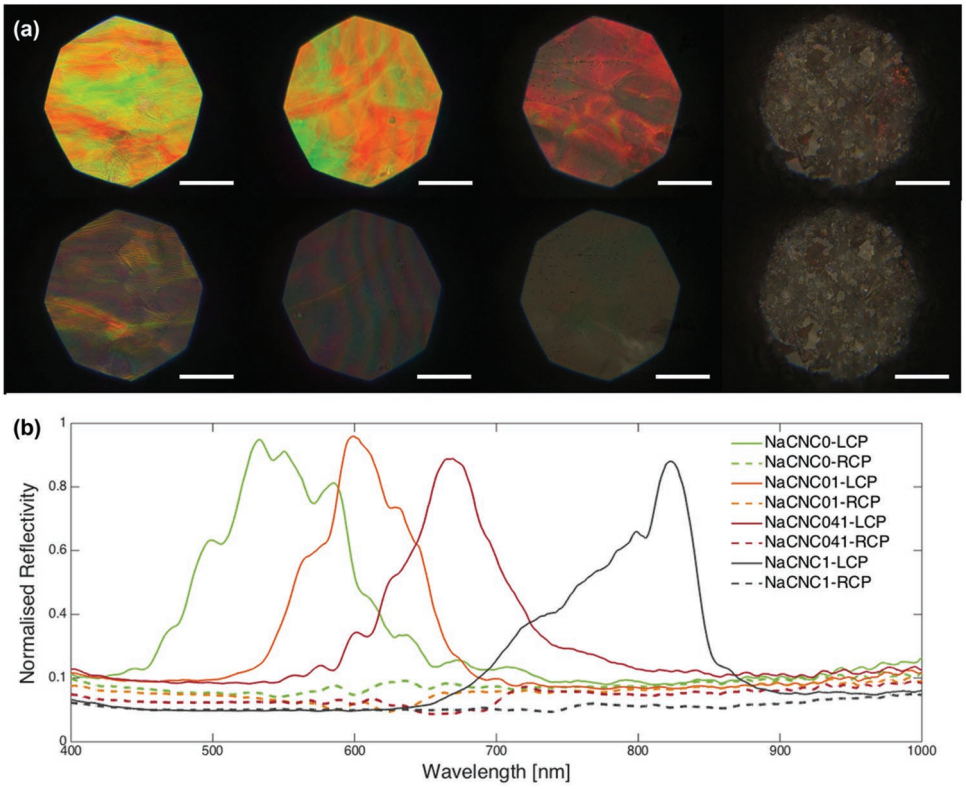

Figure 3. a) LCP (top line) and RCP (bottom line) bright field optical microscopy images and b) corresponding spectra of the pure CNC and zwitterionic surfactant CNC films prepared at 1:0, 1:0.1, 1:0.41, and 1:1 CNC:DMAPS mass ratios. Normalization is with respect to the left circular polarization channel and scale bars are 100 µm.

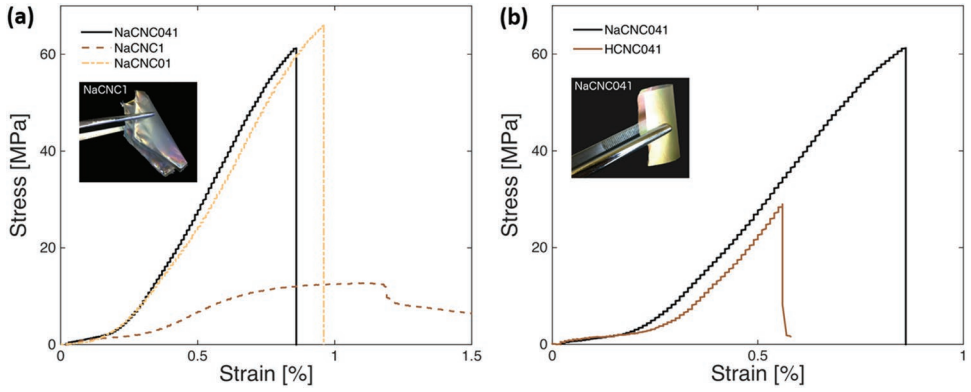

Figure 4. Stress versus strain behavior of EISA CNC-DMAPS films is dependent on a) DMAPS dosage and b) pH. Films at CNC:DMAPS = 1:1 (sample NaCNC1) and 1:0.41 (NaCNC041) show higher flexibility compared to a CNC only film and to a HCNC film with comparable amount of surfactant, respectively.

This indicates the possibility to tune the optical response of CNC films by controlling the amount of DMAPS surfactant adsorbed onto the CNC surface.

As with the optical response, the tensile strength, stiffness, and flexibility of the CNC films can be controlled via the use of DMAPS (**Figure 4**a). The zwitterionics in the films act as small springs that interact with the CNC surfaces via ionic linkages, allowing for controlled elastic-plastic deformation of the films. For the control sample (NaCNC0) it was not possible to perform a reliable and reproducible tensile stress versus strain measurement, due to the intrinsic brittleness of the films. However, for sample NaCNC01, the CNC film has an ultimate tensile strength of 63 MPa and maximum strain just below 1%. We are able to reach an ultimate tensile strength value of 13 MPa and maximum strain average of 1.2%, for sample NaCNC1. As the Zw surfactant-to-CNC ratio is increased to 1, sample NaCNC1, the response of the CNC film becomes characteristically viscoelastic, and the film is highly flexible (Figure 4a). It is worthwhile pointing out that these films are significantly stronger and more flexible than those obtained with, for instance, graphene/polyaniline composite paper or graphene paper[31a] where also the chiral nematic architecture is not always retained.[31] For graphene/polyaniline composite paper and graphene paper, it has been reported that the tensile strength was 12.6 and 8.8 MPa, and maximum strain, 0.11% and 0.08%, respectively.[31a]

Furthermore, the pH of the CNC:DMAPS suspension affects the resulting mechanical response of EISA CNC-DMAPS films. Samples NaCNC041 and HCNC041 have similar CNC:DMAPS ratios, but different pH: 4.17 and 3.04, respectively. The tensile strength and strain of the more acidic film HCNC041 were significantly lower relative to the less acidic NaCNC041 (Figure 4b). Notably, the incorporation of the Zw surfactant in the preparation of CNC films can also modulate the hardness of resulting films. Sample NaCNC01 measured a hardness similar to that to pure CNC films, and sample NaCNC041 measured 0.19 GPa, whereas sample NaCNC1 was too soft to record a measurement. It is evident that, in addition to the tensile strength and toughness properties, the hardness of CNC films can be tailored using suitable amounts of Zw surfactants to meet the needs of specific applications as in, for instance, coatings of tunable color and suitably anti-corrosive properties for automotive, high-speed trains, and aircraft.

The CNC self-assembly process strongly relies on their electrostatic interaction and therefore on their superficial charge. The addition of any other molecule in suspension will inevitably affect this interaction. This has been demonstrated in the case of small ions,[26] and also with the addition of larger molecules.[27,32] Critically, one would need to add in the suspension suitable surfactants, namely Zwitterion surfactants, that can strongly interact with the CNCs without changing the net charge surrounding them, allowing the self-assembly of CNCs into chiral nematic structures. The DMAPS maintains the same functional groups of the H_2SO_4-hydrolyzed CNCs, which are necessary for the self-assembly process. However, cationic surfactants, such as hexadecyltrimethylammonium bromide or alkyltrimethylammonium bromides (C_nTAB),[33] prevent the organization of the CNC spindles into a chiral nematic structure as they turn the net surface charge of the CNC from negative to positive.

The optical properties of the films, as evidenced by the detailed SEM, are not affected by the presence of the DMAPS, in terms of alignment of the chiral nematic director and uniformity of the pitch dimension across their volume. Dark-field measurements on the control and the CNC-DMAPS composites do not reveal significant differences in the chiral domain ordering (Figures S5 and S6, Supporting Information, ESI) but an increase in scattering for CNC-DMAPS ratio equal to 1. For CNC-DMAPS ratios larger than 0.41 (i.e., above micelle concentration), the intrinsic brittle behavior of pure CNC films remarkably change to viscoelastic. The most flexible films were obtained with CNC-DMAPS complexes having 1:1 ratio, thereby confirming that for each CNC we have at least one DMAPS mediating the interaction with neighboring ones.

In conclusion, we demonstrate the fabrication of a flexible, iridescent self-assembled CNC films using a facile, green approach. A zwitterionic surfactant, DMAPS, is adsorbed onto sulfated CNC surfaces via ionic linkages to yield nanometric CNC-DMAPS complexes. The micelles of the surfactant act as small springs that interact with the CNC surfaces. However, the cellulose nanocrystals are unperturbed, and as such retain their chiral nematic organization upon

Adv. Mater. **2016**,
DOI: 10.1002/adma.201603386

evaporation-induced self-assembly. Aqueous suspensions of these nano-complexes can also be effectively sprayed, or coated, onto essentially any surface to form cohesive, tough films. These CNC films evidently show tunable photonic and mechanical properties, whereby both properties can be tailored on the basis of zwitterionic surfactant amount and pH of the CNC suspension. The combination of tunable flexibility and iridescence can dramatically expand CNC coating and barrier film capabilities for paints and coatings applications, sustainable consumer packaging products, as well as effective templates for photonic and optelectronic materials and structures.

Experimental Section

Reagents: The zwitterionic surfactant, 3-(*N*,*N*-DMAPS ≥ 98.0% (T), sulfuric acid ACS reagent 37%, and Deuterium oxide 99.9 at% D were purchased from Sigma Aldrich. Alcohol, ACS Reagent Grade was purchased from Fisher Scientific. All chemicals were used as they are without further purification.

Preparation of CNC Suspensions: For the preparation of CNC, fully bleached, commercial kraft softwood pulp was first milled to pass through a 0.5 mm screen in a Wiley mill to ensure particle size uniformity and increase in the surface area. The milled pulp was hydrolyzed in sulfuric acid (8.75 mL of a sulfuric acid solution per gram pulp) at a concentration of 64 wt% and a temperature of 45 °C with vigorous stirring for 25 min. The cellulose suspension was then diluted with cold deionized (DI) water (≈tenfold the volume of the acid solution used) to stop the hydrolysis, and allowed to settle overnight. The clear top layer was decanted and the remaining cloudy layer was centrifuged. The supernatant was decanted and the resulting thick white suspension was washed three times with DI water to remove all soluble cellulose materials. The thick white suspension obtained after the last centrifugation step was placed inside dialysis membrane tubes (12 000–14 000 molecular weight cut-off) and dialyzed against slow running DI water, for 1–4 d. The procedure was continued until, when the membrane tubes containing the extracted cellulose materials were placed periodically in DI H_2O, the pH of the water became constant over a period of one hour. The suspension from the membrane tubes was dispersed by subjecting it to ultrasound treatment in a Fisher Sonic Dismembrator (Fisher Scientific) for 10 min at 60% power and then diluted to the desired concentration.

Preparation of CNC-Surfactant Films: 40 g of aqueous CNC suspension was mixed with 110 g of DI water and sonicated for 10 min at 60% max power in a Fisher Sonic Dismembrator (Fisher Scientific). The CNC solids content in the final suspension was 1 wt%. The CNC suspension was heated to 80 °C, and the zwitterionic surfactant, 3-(*N*,*N*-DMAPS dissolved in 50 g of DI water was added with vigorous stirring to produce suspensions with the following CNC:DMAPS mass ratios: 1:0.1, 1:0.41, and 1:1. The mixture was continuously stirred for 2 h at 80 °C until homogeneous. The clear suspension was mixed with a disintegrator for 1 min and dialyzed against DI water for 6 d until reaching a stable conductivity value. The dialyzed clear CNC-DMAPS suspensions were further sonicated for 10 min at 60% max. power using a Fisher Sonic Dismembrator, and the resulting CNC-DMAPS complex has H^+ as counter ions in suspension. The different CNC-DMAPS films used for this study were prepared by EISA. Aliquots (40 g) of the CNC-DMAPS suspensions were placed in Teflon Petri dishes (80 mm internal diameter), and allowed to evaporate at ambient conditions, under controlled air flow, on a well levelled surface. A similar protocol was used for pure CNC films.

Characterization—Elemental Analysis: Carbon, hydrogen, and nitrogen analyses were carried out in a gas chromatograph (Carlo Erba 1106), in which the sample was burned and the amount of the resulting carbon dioxide, water, and nitrogen were measured by thermal conductivity and compared directly with known standards (most commonly acetanilide and nitroaniline). Sulfur was determined by titration: after combustion, absorption, and pH adjustment, the resulting solution was titrated with standardized barium perchlorate by a volumetric method, using thorin as indicator. Elemental analyses were carried out by Canadian Microanalytical Service Ltd.

Characterization—Particle Size: An Agilent 5500 (Agilent Technologies) AFM was used in tapping mode (OTESPA-R3 tip) at room temperature to measure the CNC size distribution. The samples were prepared by drop casting 10 µL of diluted CNC suspensions on poly-L-lysine functionalized mica. After deposition the samples were rinsed with double deionized water and dried under nitrogen flow.[34] The analyzed sample area was typically 15µm × 15µm. Particle size was confirmed also by photon correlation spectroscopy (Zetasizer 3000, Malvern Instruments, UK using CNC suspensions in 1×10^{-3} M NaCl solution with 0.05% (w/w) as final CNC concentration. All runs were at least duplicated, with the reported values being the mean particle diameter for each material.

Characterization—Spectroscopy: FT-IR spectra were recorded on EISA CNC-DMAPS films using a Nicolet 6700 FT-IR spectrometer. Nuclear Magnetic Resonance (^{1}H NMR) was carried out using water suppression pulse sequence method on AV400dir spectrometer with the following settings: frequency on proton 400.13 MHz; pulse program: zggpw5; relaxation delay = 2 s; acquisition time = 2.29 s; ds = 4; number of scans was between 32 and 384 scans depending on the sample tested. ^{1}H NMR spectra were acquired directly on CNC-DMAPS suspensions.

Characterization—Polarized Light Microscopy: The films were analyzed in reflection on a customized Zeiss Axio Microscope using a Halogen lamp (Zeiss HAL100) as a light source with Koehler illumination. The light reflected off the samples passes through a quarter wave plate and a polarizing filter, specifically oriented to let only left-circularly-polarized or right-circularly-polarized light pass before being split between a CCD camera (Thorlabs DCC3240C) and an optical fibre mounted in confocal configuration and connected to a spectrometer (AvaSpec-HS2048, Avantes). This set-up allowed for the spectral acquisition from specific areas in the sample; all the spectra were normalized to the reflection of a silver mirror in one polarization channel, thus allowing for a theoretical 100% reflectivity for a perfectly chiral nematic sample in that specific channel. Dark-field images were acquired illuminating the samples from angles that are larger than the numerical aperture of the objective so that only scattered light can be collected.

Characterization—SEM Imaging: The morphological properties of the films were observed using a Leo Gemini 1530VP, Zeiss, scanning electron microscope, operated in high vacuum mode at 4 kV accelerating voltage and working distance 3–4 mm. To examine the internal structure of the EISA CNC-DMAPS films, samples were mounted on aluminum stubs, exposing the cross-section, using conductive carbon tabs, and were then sputter-coated with Au/Pd to minimize the charging effect (Emitech K550).

Characterization—Micro-Tensile Testing: Tensile mechanical measurements were performed on CNC-DMAPS films cut into rectangular strips approximately 7 mm × 25 mm, and the thickness was measured on the vertically mounted strips using a field-emission scanning electron microscope. Samples were imaged, uncoated, in low-vacuum mode. Images of the films, collected in Scandium imaging and image analysis software, were collected so that the entire film thickness is visible and the top and bottom edges of the film are discernible. Tensile testing was carried out using a Deben micro-tensile testing rig equipped with a 200 N load cell. All tensile tests were carried out at controlled conditions (23 ± 1 °C; 50 ± 2% RH). The gauge length was 10 mm and special PTFE-coated grips with textured surface were used to clamp the strip's extremities.

Characterization—Hardness Measurement: Vickers hardness measurement was carried out using a Buehler Micromet Hardness tester, Model 1600–6100. The Vickers test was performed by pressing an indenter of specified geometry into the CNC film surface. The test applies only a single test force. The resultant impression area is then

measured using a high-powered microscope. The applied force range was: 10–1000 gf. For instance, we applied 25 gf for 15 s. The CNC film to be tested was placed on a stainless steel polished surface and placed into the instrument such that it was normal to both the loading and optical axes. After the indentation test, Vickers hardness numbers were determined by measuring diagonals of the indentation using the microscope at room temperature.

Supporting Information

Supporting Information is available from the Wiley Online Library or from the author.

Acknowledgements

G.G. and S.A. contributed equally to this work. The authors thank CelluForce Inc. for funding this work, and are grateful to Drs. Richard Berry and Bruno Frka-Petesic for discussions and comments throughout the course of the project and in relation to this manuscript. S.V. acknowledges BBSRC David Phillips fellowship [BB/K014617/1] [76933] and the European Research Council [ERC-2014-STG H2020 639088], and G.G. acknowledges the EPSRC [1525292].

Received: June 27, 2016
Revised: August 12, 2016
Published online:

[1] a) K. Barta, P. C. Ford, *Acc. Chem. Res.* **2014**, *47*, 1503; b) A. K. Bledzki, J. Gassan, *Prog. Polym. Sci.* **1999**, *24*, 221; c) V. K. Thakur, M. K. Thakur, *Carbohydr. Polym.* **2014**, *109*, 102; d) M. Mariano, N. El Kissi, A. Dufresne, *J. Polym. Sci. B: Polym. Phys.* **2014**, *52*, 791.
[2] D. Klemm, P. Bertram, T. Heinze, U. Heinze, W. Wagenknecht, *Comprehensive Cellulose Chemistry*, 2nd ed., Wiley-VCH, Weinheim, Germany **2009**.
[3] a) C. Yan, J. Wang, W. Kang, M. Cui, X. Wang, C. Y. Foo, K. J. Chee, P. S. Lee, *Adv. Mater.* **2014**, *26*, 2022; b) A. G. Dumanli, G. Kamita, J. Landman, H. van der Kooij, B. J. Glover, J. J. Baumberg, U. Steiner, S. Vignolini, *Adv. Opt. Mater.* **2014**, *2*, 646.
[4] J. Cai, S. Kimura, M. Wada, S. Kuga, *Biomacromolecules* **2009**, *10*, 87.
[5] A. Mautner, K. Y. Lee, P. Lahtinen, M. Hakalahti, T. Tammelin, K. Li, A. Bismarck, *Chem. Commun.* **2014**, *50*, 5778.
[6] R. M. A. Domingues, M. E. Gomes, R. L. Reis, *Biomacromolecules* **2014**, *15*, 2327.
[7] J. Huang, H. Zhu, Y. Chen, C. Preston, K. Rohrbach, J. Cumings, L. Hu, *ACS Nano* **2013**, *7*, 2106.
[8] Z. Fang, H. Zhu, Y. Yuan, D. Ha, S. Zhu, C. Preston, Q. Chen, Y. Li, X. Han, S. Lee, G. Chen, T. Li, J. Munday, J. Huang, L. Hu, *Nano Lett.* **2013**, *14*, 765.
[9] a) Y. Habibi, *Chem. Soc. Rev.* **2014**, *43*, 1519; b) Y. Habibi, L. A. Lucia, O. J. Rojas, *Chem. Rev.* **2010**, *110*, 3479; c) M. Giese, L. K. Blusch, M. K. Khan, M. J. MacLachlan, *Angew. Chem. Int. Ed.* **2015**, DOI: 10.1002/anie.201407141; d) X. Yang, E. D. Cranston, *Chem. Mater.* **2014**, *26*, 6016; e) J. R. McKee, E. A. Appel, J. Seitsonen, E. Kontturi, O. A. Scherman, O. Ikkala, *Adv. Funct. Mater.* **2014**, *24*, 2706; f) P. Tingaut, T. Zimmermann, G. Sebe, *J. Mater. Chem.* **2012**, *22*, 20105; g) N. Lin, A. Dufresne, *Eur. Polym. J.* **2014**, *59*, 302; h) M. Jorfi, E. J. Foster, *J. Appl. Polym. Sci.* **2015**, *132*, DOI: 10.1002/app.41719; i) J. Tang, Y. Song, R. M. Berry, K. C. Tam, *RSC Adv.* **2014**, *4*, 60249; j) A. Querejeta-Fernández, G. Chauve, M. Methot, J. Bouchard, E. Kumacheva, *J. Am. Chem. Soc.* **2014**, *136*, 4788.
[10] a) B. G. Rånby, *Discuss. Faraday Soc.* **1951**, *11*, 158; b) J. F. Revol, H. Bradford, J. Giasson, R. H. Marchessault, D. G. Gray, *Int. J. Biol. Macromol.* **1992**, *14*, 170.
[11] R. H. Marchessault, F. F. Morehead, N. M. Walter, *Nature* **1959**, *184*, 632.
[12] W. H. Hamad, T. Q. Hu, *Can. J. Chem. Eng.* **2010**, *88*, 392.
[13] A. Šturcová, G. R. Davies, S. J. Eichhorn, *Biomacromolecules* **2005**, *6*, 1055.
[14] a) J.-F. Revol, D. L. Godbout, D. G. Gray, US Patent 5,629,055, **1997**; b) A. G. Dumanli, *ACS Appl. Mater. Interfaces* **2014**, *6*, 12302.
[15] K. E. Shopsowitz, H. Qi, W. Y. Hamad, M. J. MacLachlan, *Nature* **2010**, *468*, 422.
[16] K. E. Shopsowitz, W. Y. Hamad, M. J. MacLachlan, *J. Am. Chem. Soc.* **2012**, *134*, 867.
[17] J. A. Kelly, A. M. Shukaliak, C. C. Y. Cheung, K. E. Shopsowitz, W. Y. Hamad, M. J. MacLachlan, *Angew. Chem. Int. Ed.* **2013**, *52*, 8912.
[18] a) M. K. Khan, M. Giese, M. Yu, J. A. Kelly, W. Y. Hamad, M. J. MacLachlan, *Angew. Chem. Int. Ed.* **2013**, *52*, 8921; b) M. K. Khan, W. Y. Hamad, M. J. MacLachlan, *Adv. Mater.* **2014**, *26*, 2323.
[19] M. Giese, L. K. Blusch, M. K. Khan, W. Y. Hamad, M. J. MacLachlan, *Angew. Chem. Int. Ed.* **2014**, *53*, 8880.
[20] a) X. M. Dong, T. Kimura, J.-F. Revol, D. G. Gray, *Langmuir* **1996**. *12*, 2076; b) X. M. Dong, D. G. Gray, *Langmuir* **1997**, *13*, 2404.
[21] J. Pan, W. Y. Hamad, S. K. Straus, *Macromolecules* **2010**, *43*, 3851.
[22] a) S. Vignolini, P. J. Rudall, A. V. Rowland, A. Reed, E. Moyroud, R. B. Faden, J. J. Baumberg, B. J. Glover, U. Steiner, *Proc. Natl. Acad. Sci. USA* **2012**, *109*, 15712; b) M. Burresi*Sci. Rep.* **2014**, *4*, 6075 DOI:10.1038/srep06075.
[23] S. Beck, J. Bouchard, G. Chauve, R. Berry, *Cellulose* **2013**, *20*, 1401.
[24] T.-D. Nguyen, W. Y. Hamad, M. J. MacLachlan, *Chem. Commun.* **2013**, *49*, 11296.
[25] X. M. Dong, J.-F. Revol, D. G. Gray, *Cellulose* **1998**, *5*, 19.
[26] S. Beck, J. Bouchard, R. M. Berry, *Biomacromolecules* **2011**, *12*, 167.
[27] R. Bardet, N. Belgacem, J. Bras, *ACS Appl. Mater. Interfaces* **2015**, *7*, 4010.
[28] X. Zou, X. Tan, R. Berry, J. D. L. Godbout, US Patent 9,266,261, **2016**.
[29] R. Xiong, Y. Han, Y. Wang, W. Zhang, X. Zhang, C. Lu, *Carbohydr. Polym.* **2014**, *113*, 264.
[30] CNC size measured by dynamic light scattering techniques gives only the order of magnitude of the crystals, assuming they behave as spherical particles as described in the Huckel model.
[31] a) D.-W. Wang, F. Li, J. Zhao, W. Ren, Z.-G. Chen, J. Tan, Z.-S. Wu, I. Gentle, G. Q. Lu, H.-M. Cheng, *ACS Nano* **2009**, *3*, 1745; b) Q. Chen, P. Liu, C. Sheng, L. Zhou, Y. Duan, J. Zhang, *RSC Adv.* **2014**, *4*, 39301.
[32] X. Mu, D.G. Gray, *Langmuir* **2014**, *30*, 9256.
[33] C. Brinatti, J. Huang, R. M. Berry, M. K. Tam, W. Loh, *Langmuir* **2016**, *32*, 689.
[34] C. Honorato Rios, A. Kuhnhold, J. Bruckner, R. Dannert, T. Schilling, J. P. F. Lagerwall, *Front. Mater.* **2016**, *3*, 21.